Article

BEM Modeling for Stress Sensitivity of Nonlocal Thermo-Elasto-Plastic Damage Problems

Mohamed Abdelsabour Fahmy [1,2]

1 Department of Mathematics, Adham University College, Umm Al-Qura University, Adham, Makkah 28653, Saudi Arabia; maselim@uqu.edu.sa or mohamed_fahmy@ci.suez.edu.eg; Tel.: +966-5379-30306

2 Department of Basic Sciences, Faculty of Computers and Informatics, Suez Canal University, New Campus, Ismailia 41522, Egypt

Abstract: The main objective of this paper is to propose a new boundary element method (BEM) modeling for stress sensitivity of nonlocal thermo-elasto-plastic damage problems. The numerical solution of the heat conduction equation subjected to a non-local condition is described using a boundary element model. The total amount of heat energy contained inside the solid under consideration is specified by the non-local condition. The procedure of solving the heat equation will reveal an unknown control function that governs the temperature on a specific region of the solid's boundary. The initial stress BEM for structures with strain-softening damage is employed in a boundary element program with iterations in each load increment to develop a plasticity model with yield limit deterioration. To avoid the difficulties associated with the numerical calculation of singular integrals, the regularization technique is applicable to integral operators. To validate the physical correctness and efficiency of the suggested formulation, a numerical case is solved.

Keywords: boundary element method; nonlocal models; thermo-elasto-plasticity; strain-softening damage; regularization

1. Introduction

The non-classical heat conduction problem, which requires solving the parabolic heat equation under non-local conditions, is especially important here. A domain integral specifies the total amount of heat energy contained in the solid under consideration, resulting in the non-local state. The temperature is set in a specific section of the solid's border using an unknown control function to be determined. Noye et al. [1], Gumel et al. [2], Dehghan [3], and many other authors have numerically addressed this problem using finite difference methods. In the non-local case, the domain integral was reduced to an integral that only included the heat flow on the solution domain's border. The physical solution was obtained from the domain of the Laplace transformation using a computational technique for inverting Laplace transformation. Ang and Ooi [4] recently presented a boundary element technique for solving axisymmetric heat equation subject to nonlocal condition.

Continuum damage mechanics were created to fill the gap between classical continuum mechanics and fracture mechanics. Due to the presence of a fracture process zone with multiple microcracks at the fracture front, classical linear elastic fracture mechanics cannot be applied to heterogeneous quasi-brittle materials such as concrete, rocks, sea ice, fiber composites, and toughened ceramics unless very large structures are considered. Microcracking in materials eventually causes strain softening, which causes the elastic modulus matrix to become a non-positive definite, resulting in an ill-posed problem [5,6]. Finite element simulations with elasto-plastic models and yield limit deterioration in the traditional theory of plasticity produce varied findings depending on the discretization meshes [7]. The results ignore finite element mesh refinements and lead to a solution with no energy dissipation upon failure at infinite mesh refinement. To avoid this wrong

behavior, localization limiters must be implemented, ensuring that the strain-softening zone has a minimum finite size [8–13]. The non-local continuum idea, which was first presented in elasticity for a different reason [14,15], is an effective localization restriction. The non-local continuum with local strain, as proposed in References [16,17], is a useful model that treats just the elements that cause strain softening as non-local while treating all other variables as local. This idea is applicable to all constitutive models [13]. Jirásek [18] investigated non-local models, whereas Baant and Jirásek [19] conducted considerable research. The boundary element technique (BEM) is an increasingly popular alternative to the finite element method (FEM). The key advantage over domain techniques is that there are fewer unknowns. It is a powerful linear elasticity technique that has also proven useful in inelastic material challenges. Swedlow and Cruse [20] developed BEM formulations for elasto-plasticity. Ricardella [21] pioneered the initial 2D study, whereas Chaudonneret [22] and Kumar and Mukherjee [23] reported the first 2D viscoplastic analyses. Banerjee et al. also contributed to this study [24]. Banerjee and Cathie provided the first axisymmetric elasto-plastic investigations, as well as the first 3D elasto-plastic applications [25]. Since then, inelastic formulations have advanced greatly [26–29]. To resolve inelastic material difficulties, the BEM solution algorithm requires precise stress rate estimation. Regularization or singularity reduction prior to numerical computation can accelerate and improve the BEM solution process.

In this study, a novel boundary element method (BEM) modeling is utilized to numerically compute the temperature field in a body containing a preset amount of heat energy. A plasticity model with yield limit deterioration based on the regularized initial stress boundary element formulation is used to deal with non-local softening damage. This formulation eliminates one source of numerical error by utilizing a regularized integral representation of stresses. The BEM approach finally reduces the problem to a system of linear algebraic equations that need to be solved at each time level. Because of the regularization or singularity reduction performed before to numerical calculation, the validity, accuracy, and efficiency of the proposed BEM formulation are demonstrated.

2. Formulation of the Problem

According to small strain theory in the $Oxyz$ Cartesian coordinate system, the thermo-elasto-plastic governing equation can be expressed as follows [30]:

$$(\lambda_{\text{e}} + \mu)\dot{u}_{j,ji} + \mu\dot{u}_{i,jj} = \dot{\sigma}^{\text{p}}_{ij,j} \tag{1}$$

$$\frac{\partial^2\theta}{\partial x^2} + \frac{\partial^2\theta}{\partial y^2} = \frac{\rho c}{\kappa}\frac{\partial\theta}{\partial\tau} \quad \text{in } \Omega \text{ for } \tau \geqslant 0, \tag{2}$$

where

$$\dot{\sigma}^{\text{p}}_{ij} = c_{ijkl}\dot{\varepsilon}^{\text{p}}_{kl} - c_{ijkl}\dot{\theta}(x,y,\tau) \tag{3}$$

and

$$\dot{\sigma}_{ij} = c_{ijkl}\left(\dot{\varepsilon}_{kl} - \dot{\varepsilon}^{\text{p}}_{kl} - \dot{\theta}\right) = \dot{\sigma}^{\text{e}}_{ij} - \dot{\sigma}^{\text{p}}_{ij} - \dot{\theta} \tag{4}$$

Upon being subjected to the following initial, boundary, and non-local conditions,

$$u_i(x,y,0) = \dot{u}(x,y,0) = 0 \text{ in } \Omega, \tag{5}$$

$$u_i(x,y,\tau) = f_1(x,y,\tau) \text{ on } \Gamma_4 \text{ for } \tau > 0, \tag{6}$$

$$u_i(x,y,\tau) = f_2(x,y,\tau) \text{ on } \Gamma_5 \text{ for } \tau > 0, \tag{7}$$

$$t_i(x,y,\tau) = f_3(x,y,\tau) \text{ on } \Gamma_6 \text{ for } \tau > 0, \tag{8}$$

$$\theta(x,y,0) = g_0(x,y) \quad \text{in } \Omega, \tag{9}$$

$$\theta(x,y,\tau) = p(\tau)g_1(x,y) \text{ on } \Gamma_1 \text{ for } \tau > 0, \tag{10}$$

$$\theta(x,y,\tau) = g_2(x,y,\tau) \text{ on } \Gamma_2 \text{ for } \tau > 0, \tag{11}$$

$$\frac{\partial\theta}{\partial n} = g_3(x,y,\tau) \quad \text{on } \Gamma_3 \text{ for } \tau > 0, \tag{12}$$

$$\rho c \iiint_\Omega [\theta(x,y,\tau) - \theta_0] dx d\theta dy = \varepsilon(\tau) \quad \text{for } \tau > 0. \tag{13}$$

where $\Gamma_1 \cap \Gamma_2 \cap \Gamma_3 = \Gamma_4 \cap \Gamma_5 \cap \Gamma_6 = \varnothing$ such that $\Gamma_1 \cup \Gamma_2 \cup \Gamma_3 = \Gamma_4 \cup \Gamma_5 \cup \Gamma_6 = \Gamma$, $f_1(x,y,\tau)$, $f_2(x,y,\tau)$, $f_3(x,y,\tau)$ $g_0(x,y)$, $g_1(x,y)$, $g_2(x,y,\tau)$, $g_3(x,y,\tau)$, and $\varepsilon(\tau)$ are suitable chosen functions.

3. BEM Modeling of the Temperature Field

Let us consider the two-dimensional region Ω bounded by open curve Γ with endpoints A and B on the *y*-axis as shown in Figure 1.
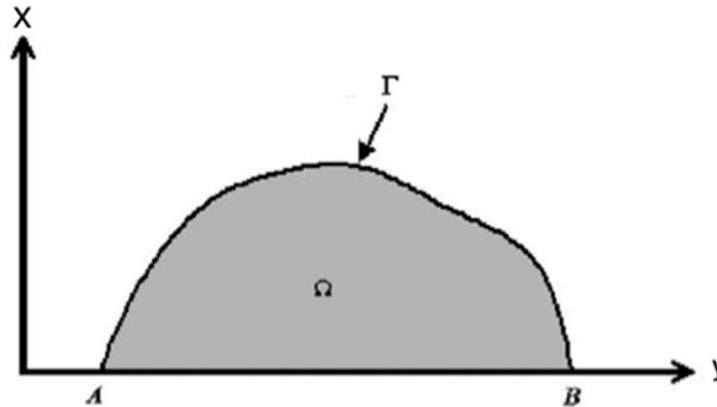

Figure 1. Model of the considered problem.

Equation (2) yields the following integro-differential equation [31]:

$$\begin{aligned}
\gamma(\xi,\eta)&\theta(\xi,\eta,\tau) \\
&= \frac{\rho c}{\kappa} \iint_\Omega G(x,y;\xi,\eta)\frac{\partial}{\partial t}[\theta(x,y,\tau)]dA(x,y) \\
&\quad + \int_\Gamma \left(\theta(x,y,\tau)\frac{\partial}{\partial n}[G(x,y;\xi,\eta)] \right. \\
&\quad \left. - G(x,y;\xi,\eta)\frac{\partial}{\partial n}[\theta(x,y,\tau)] \right) ds(x,y) \\
&\qquad \text{for}(\xi,\eta) \in \Omega \cup \Gamma,
\end{aligned} \tag{14}$$

where $\gamma(\xi,\eta) = \begin{cases} 1 \text{ if}(\xi,\eta) \in \Omega \\ \frac{1}{2} \text{ if}(\xi,\eta) \in \Gamma \end{cases}$

$$G(x,y;\xi,\eta) = -\frac{K(m(x,y;\xi,\eta))}{\pi\sqrt{a(x,y;\xi,\eta) + b(r;\xi)}}, \tag{15}$$

$$\begin{aligned}
\frac{\partial}{\partial n}[G(x,y;\xi,\eta)] = &-\frac{1}{\pi\sqrt{a(x,y;\xi,\eta) + b(x;\xi)}} \\
&\times \left\{ \frac{n_x}{2x}\left[\frac{\xi^2 - x^2 + (\eta-y)^2}{a(x,y;\xi,\eta) - b(x;\xi)}E(m(x,y;\xi,\eta)) \right. \right. \\
&\left. - K(m(x,y;\xi,\eta)) \right] \\
&\left. + n_z\frac{\eta - y}{a(x,y;\xi,\eta) - b(x;\xi)}E(m(x,y;\xi,\eta)) \right\}
\end{aligned} \tag{16}$$

$$m(x,y;\xi,\eta) = \frac{2b(x;\xi)}{a(x,y;\xi,\eta)+b(x;\xi)}, \tag{17}$$

$$a(x,y;\xi,\eta) = \xi^2 + x^2 + (\eta-y)^2, \quad b(x;\xi) = 2x\xi, \tag{18}$$

By applying the divergence theorem to (12), we obtain [32]

$$2\pi\int_\Gamma \kappa\frac{\partial}{\partial n}[\theta(x,y,\tau)]ds(x,y) = \frac{d}{d\tau}(\varepsilon(\tau)) \quad \text{for } \tau > 0. \tag{19}$$

Let $\Gamma^{(k)}$ begin and end at $\left(x^{(k)}, y^{(k)}\right)$ and $\left(x^{(k+1)}, y^{(k+1)}\right)$, respectively, and select the following two points on $\Gamma^{(k)}$ as follows

$$\left(\xi^{(k)}, \eta^{(k)}\right) = \left(x^{(k)}, y^{(k)}\right) + \tau\left(x^{(k+1)} - x^{(k)}, y^{(k+1)} - y^{(k)}\right),$$

$$\left(\xi^{(N+k)}, \eta^{(N+k)}\right) = \left(x^{(k)}, y^{(k)}\right) + (1 - \overline{\tau})\left(x^{(k+1)} - x^{(k)}, y^{(k+1)} - y^{(k)}\right), \tag{20}$$

If $\theta^{(k)}(\tau)$ and $\theta^{(N+k)}(\tau)$ are the values of temperature θ at $\left(\xi^{(k)}, \eta^{(k)}\right)$ and $\left(\xi^{(N+k)}, \eta^{(N+k)}\right)$, respectively, then the boundary temperature is approximated using

$$\theta(x, y, \tau) \simeq \frac{\left[s^{(k)}(x,y) - (1-\overline{\tau})\updownarrow^{(k)}\right]\theta^{(k)}(\tau) - \left[s^{(k)}(x,y) - \overline{\tau}\updownarrow^{(k)}\right]\theta^{(N+k)}(\tau)}{(2\overline{\tau}-1)\updownarrow^{(k)}} \tag{21}$$
$$\text{for}(x,y) \in \Gamma^{(k)}, \ 0 < \tau < \frac{1}{2}$$

where

$$s^{(k)}(x,y) = \sqrt{\left(x - x^{(k)}\right)^2 + \left(y - y^{(k)}\right)^2}. \tag{22}$$

Similarly, $q(x,y,\tau) = \partial\theta/\partial n$ is approximated using

$$q(x,y,\tau) \simeq \frac{\left[s^{(k)}(x,y) - (1-\overline{\tau})\updownarrow^{(k)}\right]q^{(k)}(\tau) - \left[s^{(k)}(x,y) - \overline{\tau}\updownarrow^{(k)}\right]q^{(N+k)}(\tau)}{(2\overline{\tau}-1)\updownarrow^{(k)}} \tag{23}$$

if $q^{(k)}(\tau) = q\left(\xi^{(k)}, \eta^{(k)}, \tau\right)$ and $q^{(N+k)}(\tau) = q\left(\xi^{(N+k)}, \eta^{(N+k)}, \tau\right)$.

The integro-differential Equation (14) can be approximated as [33]

$$\begin{aligned}
\gamma(\xi, \eta)\, \theta(\xi, \eta, \tau) \\
= \frac{\rho c}{\kappa}\iint_\Omega (x, y; \xi, \eta)\frac{\partial}{\partial t}[\theta(x,y,\tau)]\mathrm{d}A(x,y) \\
+ \sum_{k=1}^{N}\frac{1}{(2\overline{\tau}-1)\updownarrow^{(k)}}\left\{\left[-(1-\overline{\tau})\updownarrow^{(k)}\mathcal{F}_2^{(k)}(\xi,\eta)\right.\right. \\
\left.+ \mathcal{F}_4^{(k)}(\xi,\eta)\right]\theta^{(k)}(\tau) \\
+ \left[\tau\updownarrow^{(k)}\mathcal{F}_2^{(k)}(\xi,\eta) - \mathcal{F}_4^{(k)}(\xi,\eta)\right]\theta^{(N+k)}(\tau) \\
- \left[-(1-\overline{\tau})\updownarrow^{(k)}\mathcal{F}_1^{(k)}(\xi,\eta) + \mathcal{F}_3^{(k)}(\xi,\eta)\right]q^{(k)}(\tau) \\
\left.- \left[\tau\updownarrow^{(k)}\mathcal{F}_1^{(k)}(\xi,\eta) - \mathcal{F}_3^{(k)}(\xi,\eta)\right]q^{(N+k)}(\tau)\right\},
\end{aligned} \tag{24}$$

$$\mathcal{F}_1^{(k)}(\xi,\eta) = \int_{\Gamma^{(k)}} G(x,y;\xi,\eta)x\mathrm{d}s(x,y), \tag{25}$$

$$\mathcal{F}_2^{(k)}(\xi,\eta) = \int_{\Gamma^{(k)}} \frac{\partial}{\partial n}[G(x,y;\xi,\eta)]x\mathrm{d}s(x,y), \tag{26}$$

$$\mathcal{F}_3^{(k)}(\xi,\eta) = \int_{\Gamma^{(k)}} s(x,y)G(x,y;\xi,\eta)x\mathrm{d}s(x,y), \tag{27}$$

$$\mathcal{F}_4^{(k)}(\xi,\eta) = \int_{\Gamma^{(k)}} s(x,y)\frac{\partial}{\partial n}[G(x,y;\xi,\eta)]x\mathrm{d}s(x,y). \tag{28}$$

The domain integral in (24) is approximated by picking L collocation points $\left(\xi^{(2N+1)}, \eta^{(2N+1)}\right), \left(\xi^{(2N+2)}, \eta^{(2N+2)}\right), \ldots, \left(\xi^{(2N+L-1)}, \eta^{(2N+L-1)}\right), \left(\xi^{(2N+L)}, \eta^{(2N+L)}\right)$ within the interior of Ω. As collocation points on the element $\Gamma^{(k)}(k = 1, 2, \ldots, N)$, the points $\left(\xi^{(k)}, \eta^{(k)}\right)$ and $\left(\xi^{(N+k)}, \eta^{(N+k)}\right)$ are also used. Thus, we obtain

$$\iint_\Omega G(x,y;\xi,\eta)\frac{\partial}{\partial\tau}[\theta(x,y,\tau)]dA(x,y) \simeq \sum_{k=1}^{2N+P}\frac{d}{d\tau}\left[\theta^{(k)}(\tau)\right]\sum_{j=1}^{2N+P}W^{(kj)}\Psi^{(j)}(\xi,\eta), \quad (29)$$

where $\theta^{(k)}(t) = \theta\left(\xi^{(k)},\eta^{(k)}\right)$ for $k = 1,2,\ldots,2N+L$, the coefficients $W^{(kj)}$ are defined implicitly by [34]

$$\sum_{j=1}^{2N+L}W^{(kj)}\phi^{(p)}\left(\xi^{(j)},\eta^{(j)}\right) = \begin{cases} 0 & \text{if } p \neq k \\ 1 & \text{if } p = k \end{cases} \text{ for } p,\ k = 1,2,\ldots,2N+L \quad (30)$$

and

$$\Psi^{(j)}(\xi,\eta) = \gamma(\xi,\eta)\chi^{(j)}(\xi,\eta) + \int_\Gamma xG(x,y;\xi,\eta)\frac{\partial}{\partial n}\left[\chi^{(j)}(\xi,\eta)\right]ds(x,y)$$
$$-\int_\Gamma x\chi^{(j)}(\xi,\eta)\frac{\partial}{\partial n}[G(x,y;\xi,\eta)]ds(x,y) \text{ for } j = 1,2,\ldots,2N+L \quad (31)$$

$$\phi^{(p)}(x,y) = 4E\left(m\left(x,y;\ \xi^{(p)},\ \eta^{(p)}\right)\right)\sqrt{a\left(x,y;\ \xi^{(p)},\ \eta^{(p)}\right) + b\left(r;\ \xi^{(p)}\right)}, \quad (32)$$

$$\chi^{(p)}(\xi,\eta) = \frac{1}{9}\left(a\left(x,y;\ \xi^{(p)},\ \eta^{(p)}\right) + b\left(x;\xi^{(p)}\right)\right)\sqrt{a\left(x,y;\ \xi^{(p)},\ \eta^{(p)}\right) + b\left(x;\ \xi^{(p)}\right)}$$
$$\times\left[\left(m\left(x,y;\ \xi^{(p)},\ \eta^{(p)}\right) - 1\right)K\left(m\left(x,y;\ \xi^{(p)},\ \eta^{(p)}\right)\right)\right]$$
$$\left[+\left(4 - 2m\left(x,y;\ \xi^{(p)},\ \eta^{(p)}\right)\right)E\left(m\left(x,y;\ \xi^{(p)},\ \eta^{(p)}\right)\right)\right] \quad (33)$$

Thus, we use the following approximations:

$$\theta^{(k)}(\tau) \simeq \frac{1}{2}\left[\theta^{(k)}\left(\tau + \frac{1}{2}\Delta\tau\right) + \theta^{(k)}\left(\tau - \frac{1}{2}\Delta\tau\right)\right],$$
$$\frac{d}{dt}\left[\theta^{(k)}(\tau)\right] \simeq \frac{1}{\Delta\tau}\left[\theta^{(k)}\left(\tau + \frac{1}{2}\Delta\tau\right) - \theta^{(k)}\left(\tau - \frac{1}{2}\Delta\tau\right)\right], \quad (34)$$

Then, from (29) and (24), we obtain

$$\frac{1}{2}\gamma\left(\xi^{(n)},\eta^{(n)}\right)\left[\theta^{(n)}\left(\tau + \frac{1}{2}\Delta\tau\right) + \theta^{(n)}\left(\tau - \frac{1}{2}\Delta\tau\right)\right]$$
$$= \frac{\rho c}{\kappa\Delta\tau}\sum_{k=1}^{2N+P}\left[\theta^{(k)}\left(\tau + \frac{1}{2}\Delta\tau\right) - \theta^{(k)}\left(\tau - \frac{1}{2}\Delta\tau\right)\right]$$
$$\times\sum_{j=1}^{2N+P}W^{(kj)}\Psi^{(j)}\left(\xi^{(n)},\eta^{(n)}\right)$$
$$+\sum_{k=1}^{N}\frac{1}{(2\overline{\tau}-1)\updownarrow^{(k)}}\left\{\frac{1}{2}\left[-(1-\overline{\tau})\updownarrow^{(k)}\mathcal{F}_2^{(k)}\left(\xi^{(n)},\eta^{(n)}\right)\right.\right.$$
$$+\mathcal{F}_4^{(k)}\left(\xi^{(n)},\eta^{(n)}\right)\left]\left[\theta^{(k)}\left(\tau + \frac{1}{2}\Delta\tau\right) + \theta^{(k)}\left(\tau + \frac{1}{2}\Delta\tau\right)\right]\right.$$
$$+\frac{1}{2}\left[\tau\updownarrow^{(k)}\mathcal{F}_2^{(k)}\left(\xi^{(n)},\eta^{(n)}\right) - \mathcal{F}_4^{(k)}\left(\xi^{(n)},\eta^{(n)}\right)\right]$$
$$\times\left[\theta^{(N+k)}\left(\tau + \frac{1}{2}\Delta\tau\right) + \theta^{(N+k)}\left(\tau + \frac{1}{2}\Delta\tau\right)\right]$$
$$-\left[-(1-\overline{\tau})\updownarrow^{(k)}\mathcal{F}_1^{(k)}\left(\xi^{(n)},\eta^{(n)}\right) + \mathcal{F}_3^{(k)}\left(\xi^{(n)},\eta^{(n)}\right)\right]q^{(k)}$$
$$-\left[\tau\updownarrow^{(k)}\mathcal{F}_1^{(k)}\left(\xi^{(n)},\eta^{(n)}\right) - \mathcal{F}_3^{(k)}\left(\xi^{(n)},\eta^{(n)}\right)\right]q^{(N+k)}\right\}$$
$$\text{for } n = 1,2,\ldots,2N+L. \quad (35)$$

If the temperature is provided by either (10) or (11) at $\left(\xi^{(k)},\eta^{(k)}\right)(k = 1,2,\ldots,2N)$, then $q^{(k)}(\tau)$ is not known. In the event where the temperature's normal derivative is provided by (12) at $\left(\xi^{(k)},\eta^{(k)}\right)(k = 1,2,\ldots,2N)$, then $\theta^{(k)}(\tau)$ is not known. At every L inner collocation point, the temperature is unknown.

In other words, (35) represents a system of $2N+L$ linear algebraic equations in $2N+L+1$ unknown functions of τ if $\theta^{(n)}\left(\tau - \frac{1}{2}\Delta\tau\right)(n = 1,2,\ldots,2N+L)$ is taken to be known. (Remember that the control function $p(\tau)$, which is shown in (10), is an unidentified

function that needs to be found). Therefore, the system requires one further equation to be completed.

Using (23), Equation (19) can be expressed as

$$2\pi\kappa\sum_{k=1}^{N}\left[\mathcal{H}_1^{(k)}-(1-\overline{\tau})\mathcal{H}_2^{(k)}\right]\left(q^{(k)}+q^{(N+k)}\right)=\frac{\mathrm{d}}{\mathrm{d}t}[\varepsilon(\tau)], \tag{36}$$

where

$$\mathcal{H}_1^{(k)}=\frac{1}{(2\overline{\tau}-1)}\left(\frac{1}{2}\updownarrow^{(k)}x^{(k)}+\frac{1}{3}\left[\updownarrow^{(k)}\right]^2n_y^{(k)}\right), \tag{37}$$

$$\mathcal{H}_2^{(k)}=\frac{1}{(2\overline{\tau}-1)}\left(\updownarrow^{(k)}x^{(k)}+\frac{1}{2}\left[\updownarrow^{(k)}\right]^2n_y^{(k)}\right). \tag{38}$$

The steps to solve the linear algebraic Equations (35) and (36) are as follows:

Step 1 Let $\tau=\frac{1}{2}\Delta\tau$ in (35) and (36).

Step 2 Determine $\theta^{(k)}(0)(k=1,2,\ldots,2N+L)$ using the initial condition in (2a).

Step 3 Solve the linear algebraic Equations (35) and (36) for the unknowns $p\left(\frac{1}{2}\Delta\tau\right)$, $\theta^{(2N+k)}(\Delta\tau)(k=1,2,\ldots,L)$, and either $\theta^{(i)}(\Delta\tau)$ or $q^{(i)}\left(\frac{1}{2}\Delta\tau\right)(i=1,2,\ldots,2N)$.

Step 4 With $\theta^{(k)}(\Delta\tau)(k=1,2,\ldots,2N+L)$ now known and $\tau=\frac{3}{2}\Delta\tau$ in (35) and (36),

Step 5 Solve linear algebraic Equations (35) and (36) for the unknowns $p(\frac{3}{2}\Delta\tau)$, $\theta^{(2N+k)}(2\Delta\tau)(k=1,2,\ldots,L)$, and either $\theta^{(i)}(2\Delta\tau)$ or $q^{(i)}(\frac{3}{2}\Delta\tau)(i=1,2,\ldots,2N)$.

Step 6 By repeatedly letting $\tau=\frac{5}{2}\Delta\tau,\ \frac{7}{2}\Delta\tau,\ \frac{9}{2}\Delta\tau,\ldots\ldots$, at higher time levels, it is possible to solve for unknowns.

4. BEM Modeling of Thermo-Elasto-Plastic Deformation

The integral equation for the displacement rate is as follows [35]:

$$\dot{u}_j(y)=\int_{\Omega}\dot{\sigma}_{ik}^{\mathrm{P}}(x)U_{ikj}(x-y)\mathrm{d}\Omega+\int_{\Gamma}\dot{t}_i(\eta)U_{ij}(\eta-y)\mathrm{d}\Gamma-\int_{\Gamma}\dot{u}_i(\eta)T_{ij}(\eta,y)\mathrm{d}\Gamma \tag{39}$$

where the fundamental displacement U_{ij} must satisfy the following equation

$$c_{ijkl}U_{km,jl}(x-y)=-\delta_{im}\delta(x-y)\qquad(y\in\Omega) \tag{40}$$

The other kernel functions of Equation (39) are as follows [35]

$$T_{ij}(\eta,y)=c_{isml}n_s(\eta)U_{mj,l}(\eta-y) \tag{41}$$

$$U_{ikj}(x-y)=U_{ij,k} \tag{42}$$

where

$$U_{ik}(x-y)=\frac{1}{8\pi\mu(1-v)}[-(3-4v)\delta_{ik}\ln r+r_{,i}r_{,k}] \tag{43}$$

$$T_{ik}(x,y)=\frac{1-2v}{4\pi(1-v)r}\left[r_kn_i(x)-r_{,i}n_k(x)-\left(\delta_{ik}+\frac{2}{1-2v}r_{,i}r_{,k}\right)r_{,j}n_j(x)\right] \tag{44}$$

$$U_{ijk}(x-y)=\frac{1-2v}{4\pi\mu(1-v)r}\left[(1-2v)\left(r_{,j}\delta_{ik}+r_{,i}\delta_{jk}\right)-r_{,k}\delta_{ij}+2r_{,i}\,r_{,j}\,r_{,k}\right] \tag{45}$$

$$D_{lji}(x-y)=\frac{1}{4\pi(1-v)r}\left[(1-2v)\left(r_{,j}\delta_{li}+r_{,l}\delta_{ji}-r_{,i}\delta_{lj}\right)+2r_{,i}\,r_{,j}\,r_{,l}\right] \tag{46}$$

$$\begin{aligned}T_{ljim}(x-y)=&\frac{\mu}{4\pi(1-v)r}\left\{4v\delta_{lj}\varepsilon_{kim}r_{,k}\right.\\&+(1-2v)\left[r_{,l}\varepsilon_{jim}+r_{,j}\varepsilon_{lim}-r_{,k}\left(\delta_{il}\varepsilon_{jkm}+\delta_{ij}\varepsilon_{lkm}\right)\right]\\&\left.-2r_{,i}r_{,k}\left(r_{,l}\varepsilon_{jkm}+r_{,j}\varepsilon_{lkm}\right)\right\}\end{aligned} \tag{47}$$

$$\begin{aligned}E_{ijkl}(x-y)=&\frac{1}{4\pi(1-v)r^2}\left\{(1-2v)\left(\delta_{il}\delta_{jk}+\delta_{ik}\delta_{jl}-\delta_{ij}\delta_{kl}+2\delta_{ij}r_{,k}r_{,l}\right)+2\,\delta_{kl}\,r_{,i}\,r_{,j}\right.\\&\left.+2v\left(\delta_{ik}r_{,j}r_{,l}+\delta_{il}r_{,j}r_{,k}+\delta_{jk}r_{,i}r_{,l}+\delta_{jl}r_{,i}r_{,k}\right)-8r_{,i}\,r_{,j}\,r_{,k}\,r_{,l}\right\}\end{aligned} \tag{48}$$

in which

$$r_i = x_i - y_i, r = (r_i r_i)^{\frac{1}{2}}, r_{,i} = \frac{r_i}{r} \tag{49}$$

As a result, we have the following boundary integral equation (BIE)

$$\int_{\Gamma} \left[\dot{u}_i(\eta) - \dot{u}_i(\zeta) \right] T_{ij}(\eta, \zeta) \mathrm{d}\Gamma - \int_{\Gamma} \dot{t}_i(\eta) U_{ij}(\eta - \zeta) \mathrm{d}\Gamma = \int_{\Omega} \dot{\sigma}_{ik}^{\mathrm{P}}(x) U_{ikj}(x - \zeta) \mathrm{d}\Omega \tag{50}$$

Upon substituting the displacement rate integral Equation (39) into (4) and applying regularization [36], we obtain the following stress rate integral equation

$$\dot{\sigma}_{ij}(y) = -\dot{\sigma}_{ij}^{\mathrm{P}}(y) + c_{ijms} \frac{\partial}{\partial y_s} \int_{\Omega} \dot{\sigma}_{kl}^{\mathrm{P}}(x) U_{km,l}(x - y) \mathrm{d}\Omega$$
$$+ \int_{\Gamma} \left[\dot{t}_k(\eta) D_{ijk}(\eta - y) + T_{ijkl}(\eta - y) \widehat{D}_l \dot{u}_k(\eta) \right] \mathrm{d}\Gamma. \tag{51}$$

where

$$\widehat{D}_l = \delta_{l3} \frac{\partial}{\partial \tau}(\eta) \tag{52}$$

where $\tau(\eta)$ is the unit vector tangent to Γ at η.

To treat a strong singularity of the kernel, the domain Ω can be split into regular and singular parts, $\Omega = \Omega_{\mathrm{R}} + \Omega_{\mathrm{S}}$; thus, we can write

$$\dot{\sigma}_{ij}(y) = -\dot{\sigma}_{ij}^{\mathrm{P}}(y) + \int_{\Omega} \left[\dot{\sigma}_{kl}^{\mathrm{P}}(x) - \dot{\sigma}_{kl}^{\mathrm{P}}(y) \right] E_{ijkl}(x - y) \mathrm{d}\Omega + \int_{\Gamma} \left[\dot{t}_k(\eta) D_{ijk}(\eta - y) \right.$$
$$\left. + T_{ijkl}(\eta - y) \widehat{D}_l \dot{u}_k(\eta) \right] \mathrm{d}\Gamma + \dot{\sigma}_{kl}^{\mathrm{P}}(y) \left[\int_{\Omega_{\mathrm{R}}} D_{ijk,l}(x - y) \mathrm{d}\Omega + A_{ijkl} \right] \tag{53}$$

With

$$E_{ijkl} = -c_{ijps} U_{kp,ls} = D_{ijk,l} \tag{54}$$

$$A_{ijkl} = \mathrm{CPV} \int_{\Omega_{\mathrm{S}}} D_{ijk,l}(x - y) \mathrm{d}\Omega, \quad y \notin \Omega_{\mathrm{R}}, \quad y \in \Omega_{\mathrm{S}} \tag{55}$$

where

$$A_{ijkl} = \frac{1}{8(1 - v)} \left[(3 - 4v)\left(\delta_{ik}\delta_{jl} + \delta_{il}\delta_{jk} \right) - (1 - 4v)\delta_{ij}\delta_{kl} \right] \tag{56}$$

The BIE (53) can be used to estimate the stress tensor rates as follows

$$\dot{\sigma}_{ij}(\zeta) = c_{ijkl}\dot{u}_{k,l}(\zeta) - \dot{\sigma}_{ij}^{\mathrm{P}}(\zeta) \tag{57}$$

By solving the regularized BIE [37], with using (51), we obtain

$$\dot{\sigma}_{ij}(y) + \dot{\sigma}_{ij}^{\mathrm{P}}(y) = \left(\dot{\sigma}_{kl}(y) + \dot{\sigma}_{kl}^{\mathrm{P}}(y) \right) \int_{\Gamma} n_l(\eta) D_{ijk}(\eta - y) \mathrm{d}\Gamma$$
$$+ \dot{u}_{k,l}(y) \int_{\Gamma} \tau_l(\eta) T_{ijk3}(\eta - y) \mathrm{d}\Gamma. \tag{58}$$

Thus, by using (51), we have the following relations

$$\dot{\sigma}_{ij}^{\mathrm{P}}(x) = 0, \dot{\tilde{\sigma}}_{ij}(x) = c_{ijkl}\dot{\tilde{u}}_{k,l}(x) = c_{ijkl}\dot{u}_{k,l}(y) = \dot{\sigma}_{ij}(y) + \dot{\sigma}_{ij}^{\mathrm{P}}(y) \tag{59}$$

Using the subtraction and addition technique [38] and $y = \zeta \in \Gamma$ for the regularized BIE, we obtain

$$\dot{u}_{k,l}(\zeta) \sum_p \mathrm{and} \int_{\Gamma_p} \lfloor \tau_l(\eta) - \hat{\chi}_p \tau_l(\zeta) \rfloor T_{ijk3}(\eta - \zeta) \mathrm{d}\Gamma$$
$$+ \dot{\sigma}_{kl}(\zeta) \sum_p \int_{\Gamma_p} \lfloor n_l(\eta) - \hat{\chi}_p n_l(\zeta) \rfloor D_{ijk}(\eta - \zeta) \mathrm{d}\Gamma$$
$$= \int_{\Omega} \left[\dot{\sigma}_{kl}^{\mathrm{P}}(x) - \dot{\sigma}_{kl}^{\mathrm{P}}(\zeta) \right] E_{ijkl}(x - \zeta) \mathrm{d}\Omega + \sum_p \int_{\Gamma_p} \left[t_k(\eta) - \hat{\chi}_p t_k(\zeta) \right] D_{ijk}(\eta - \zeta) \mathrm{d}\Gamma$$
$$+ \sum_p \int_{\Gamma_p} \left[\frac{\partial u_k}{\partial \tau}(\eta) - \hat{\chi}_p \frac{\partial u_k}{\partial \tau}(\zeta) \right] T_{ijk3}(\eta - \zeta) \mathrm{d}\Gamma \tag{60}$$

where

$$\widehat{\chi}_p f(\zeta) = \begin{cases} l \, f(\eta), & \zeta \in \Gamma_p \\ \Gamma_p \in \eta \to \zeta & \\ 0, & \zeta \notin \Gamma_p \end{cases} \tag{61}$$

The incremental iterative solution approach will employ the regularized BIE (50) and (60) as well as the regularized BIE (53). Thus, the regular Gaussian quadrature rule has been used to calculate all the boundary and domain integrals.

The yield function can be expressed as

$$F(\sigma_{ij}, k) = f(\sigma_{ij}) - \psi(k) = 0 \tag{62}$$

For the model in this study, the work-hardening function is used to characterize softening, where the hardening/softening parameter k the plastic strain increment $d\varepsilon_{ij}^{\mathrm{p}}$ can be defined as

$$k = \int \sigma_{ij} d\varepsilon_{ij} \tag{63}$$

$$d\varepsilon_{ij}^{\mathrm{p}} = d\lambda a_{ij} \tag{64}$$

where $a_{ij} = \partial F / \partial \sigma_{ij}$.

From (62) and (64), the proportionality coefficient $d\lambda$ can be expressed as

$$d\lambda = \frac{a_{ij} c_{ijkl} d\varepsilon_{kl}}{a_{ij} a_{kl} c_{ijkl} + (d\psi/dk)\sigma_{ij} a_{ij}} \tag{65}$$

We will consider the strain-softening von Mises plasticity model in this work because the nonlocal BEM solution will be easier and more obvious.

The stress intensity

$$\sigma_e = \left(\frac{3}{2} s_{ij} s_{ij}\right)^{1/2} \tag{66}$$

in which

$$s_{ij} = \sigma_{ij} - \frac{1}{3}\delta_{ij}\sigma_{kk}, \tag{67}$$

and

$$\sigma_e - \sigma_0(k) = 0. \tag{68}$$

Thus, we obtain

$$d\varepsilon_{ij}^{\mathrm{p}} = \frac{3}{2} \frac{s_{ij}}{\sigma_e} d\lambda. \tag{69}$$

$$d\lambda = 3\mu \frac{s_{kl}}{3\mu + H} \frac{d\varepsilon_{kl}}{\sigma_e} \tag{70}$$

where

$$H = d\psi/d\varepsilon^{\mathrm{p}} \tag{71}$$

and

$$\varepsilon^{\mathrm{p}} = \left(\frac{2}{3}\varepsilon_{ij}^{\mathrm{p}}\varepsilon_{ij}^{\mathrm{p}}\right)^{1/2} \tag{72}$$

The fundamental idea behind the non-local continuum is that only the constitutive equation variables that cause strain softening are non-local [7]. Spatial averaging is more computationally efficient than plastic strains

Then, the non-local scaling parameter $d\bar{\lambda}$ can be defined as

$$d\bar{\lambda}(y) = \frac{1}{V_\alpha(y)} \int_\Omega \alpha(x,y) d\lambda(x) d\Omega(x) \tag{73}$$

where

$$V_\alpha(y) = \int_\Omega \alpha(x,y) d\Omega(x) \tag{74}$$

where the non-local weight function $\alpha(x,y)$ can be expressed as [7]

$$\alpha(x,y) = \exp\left(-\left(2r/l\right)^2\right) \tag{75}$$

where l measures the material heterogeneity scale and $r = |x - y|$.

After determining the non-local average $\mathrm{d}\bar{\lambda}$, we can calculate the non-local plastic strain and stress increments as follows

$$\mathrm{d}\bar{\varepsilon}_{ij}^{\mathrm{P}} = \mathrm{d}\bar{\lambda} a_{ij} \tag{76}$$

$$\mathrm{d}\bar{\sigma}_{ij}^{\mathrm{P}} = \mathrm{d}\bar{\lambda} a_{kl} c_{ijkl} \tag{77}$$

The BIE (50) can be transformed into matrix form using the discretization in the BEM formulation as

$$\mathbf{T}\dot{\mathbf{u}} = \mathbf{U}\dot{\mathbf{t}} + \mathbf{Q}\dot{\sigma}^{\mathrm{P}} \tag{78}$$

The stress tensor rates can be expressed as

$$\dot{\sigma} = \mathbf{D}\dot{\mathbf{t}} + \mathbf{T}'\dot{\mathbf{u}} + \mathbf{E}\dot{\sigma}^{\mathrm{P}} \tag{79}$$

Thus, we can write (78) and (79) as follows

$$\mathbf{A}\,\dot{\mathbf{X}} = \dot{\mathbf{F}} + \mathbf{Q}\dot{\sigma}^{\mathrm{P}} \tag{80}$$

$$\dot{\sigma} = \mathbf{A}'\dot{\mathbf{X}} + \dot{\mathbf{F}}' + \mathbf{E}\dot{\sigma}^{\mathrm{P}} \tag{81}$$

Then, the boundary unknowns are

$$\dot{\mathbf{X}} = \mathbf{R}\dot{\sigma}^{\mathrm{P}} + \dot{\mathbf{M}} \tag{82}$$

where

$$\mathbf{R} = \mathbf{A}^{-1}\mathbf{Q}, \qquad \dot{\mathbf{M}} = \mathbf{A}^{-1}\dot{\mathbf{F}} \tag{83}$$

By using (81) and (82), the plastic stress rate can be expressed as

$$\dot{\sigma}^{\mathrm{e}} = \mathbf{S}\dot{\sigma}^{\mathrm{P}} + \dot{\mathbf{N}} \tag{84}$$

where

$$\mathbf{S} = \mathbf{E} + \mathbf{I} + \mathbf{A}'\mathbf{R} \tag{85}$$

$$\dot{\mathbf{N}} = \dot{\mathbf{F}}' + \mathbf{A}'\dot{\mathbf{M}} \tag{86}$$

The iteration process may be summarized as follows:

Step 1 Calculate $\mathrm{d}\sigma_{ij}^{\mathrm{e}}$ from (84);

Step 2 Calculate $\mathrm{d}\lambda = \dfrac{a_{ij}\mathrm{d}\sigma_{ij}^{\mathrm{e}}}{a_{ij}a_{kl}c_{ijkl} + (\mathrm{d}\psi/\mathrm{d}k)\sigma_{ij}a_{ij}}$;

Step 3 Calculate $\mathrm{d}\bar{\lambda}$ from (73);

Step 4 Calculate $\mathrm{d}\bar{\sigma}_{ij}^{\mathrm{P}} = \mathrm{d}\bar{\lambda} c_{ijkl} a_{kl}$;

Step 5 Verify iteration convergence by comparing $\mathrm{d}\sigma_{ij}^{\mathrm{P}}$ to the value of (84) in step 1;

Step 6 If the relative change between two subsequent iteration stages is less than the set tolerance (which is a value obtained by measuring a component's capacity to perform its design function in the presence of a flaw or damage), return to step 1 and start a new load increment.

5. Numerical Results and Discussion

The proposed BEM strategy employed in this study can be used for a broad spectrum of thermal stress sensitivity of nonlocal thermo-elasto-plastic damage problems.

To solve the systems resulting from the BEM discretization in the current study, we employed Zan et al.'s stable communication avoidance S-step-generalized minimal residual approach (SCAS-GMRES) to reduce the number of iterations and computation time [39]. Table 1 compares the SCAS-GMRES [39], fast modified diagonal, and toeplitz splitting (FMDTS) of Xin and Chong [40] and the unconditionally convergent-scaled circulant and skew-circulant splitting (UC-RSCSCS) of Zi et al. [41] during our solution of the current problem. This table displays the number of iterations (Iter.), processor time (CPU time), relative residual (Rr), and error (Err.) calculated for various length scale parameter values ($l = 0.01$, 0.1, and 1.0). According to Table 1, the SCAS-GMRES iterative approach uses

the least amount of Iter. and CPU time, meaning that it outperforms the FMDTS and UC-RSCSCS iterative methods.

Table 1. Numerical results for the considered iteration methods.

l	Method	Iter.	CPU Time	Rr	Err.
	SCAS-GMRES	40	0.0123	1.84e−07	1.62e−09
0.01	FMDTS	70	0.0567	6.62e−07	1.84e−07
	UC-RSCSCS	80	0.0795	8.42e−07	2.56e−06
	SCAS-GMRES	50	0.0594	0.16e−06	2.12e−08
0.1	FMDTS	100	0.2278	1.68e−05	4.25e−06
	UC-RSCSCS	140	0.3784	1.09e−04	0.48e−05
	SCAS-GMRES	60	0.1768	2.45e−05	1.74e−07
1.0	FMDTS	280	0.7948	1.76e−04	3.82e−05
	UC-RSCSCS	300	0.8964	1.34e−03	4.54e−04

The thermal stresses σ_{11}, σ_{12}, and σ_{22} sensitivities are compared for various softening damage parameters ($Z = -1000$ MPa and $Z = -3000$ MPa) concerning the differences between local and non-local theories

Figure 2 shows that the values of the thermal stress σ_{11} sensitivity based on the softening parameter $Z = -1000$ MPa are larger compared to the values based on the softening parameter $Z = -3000$ MPa for local and nonlocal theories. The values of the thermal stress σ_{11} sensitivity based on the softening parameters $Z = -1000$ MPa and $Z = -3000$ MPa decrease in the range $0 \leq x_1 \leq 0.4$ and increase in the range $0.4 \leq x_1 \leq 1.5$. However, the values of the thermal stress σ_{11} sensitivity based on the softening parameters $Z = -1000$ MPa and $Z = -3000$ MPa converge to zero with increasing x_1 for $x_1 \geq 1.5$.

Figure 3 shows that the values of the stress σ_{12} sensitivity in both softening parameters $Z = -1000$ MPa and $Z = -3000$ MPa decrease in the ranges $0 \leq x_1 \leq 0.2$ and $0.7 \leq x_1 \leq 1.5$ for local theory, while increasing in the range $0.2 \leq x_1 \leq 0.7$. However, for nonlocal theory, the values of the stress σ_{12} sensitivity based on softening parameter $Z = -1000$ MPa increase in the range $0 \leq x_1 \leq 1$ and decrease in the range $1 \leq x_1 \leq 1.5$, while, based on the softening parameter $Z = -1000$ MPa, decrease in the range $0 \leq x_1 \leq 0.3$ and increase in the range $0.3 \leq x_1 \leq 1.5$. The values of the stress σ_{12} sensitivity based on the softening parameters $Z = -1000$ MPa and $Z = -3000$ MPa converge to zero with increasing x_1 for $x_1 \geq 1.5$.
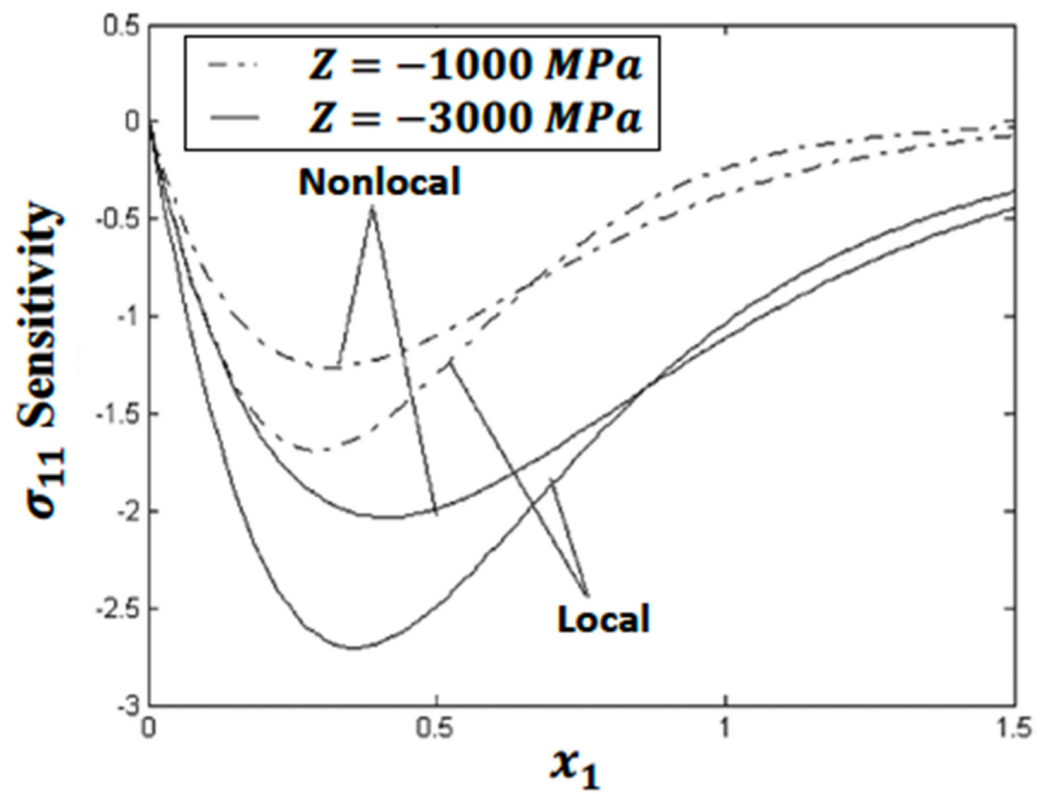
Figure 2. Variation in the thermal stress σ_{11} sensitivity along the x_1-axis for two different softening parameters of local and nonlocal theories.
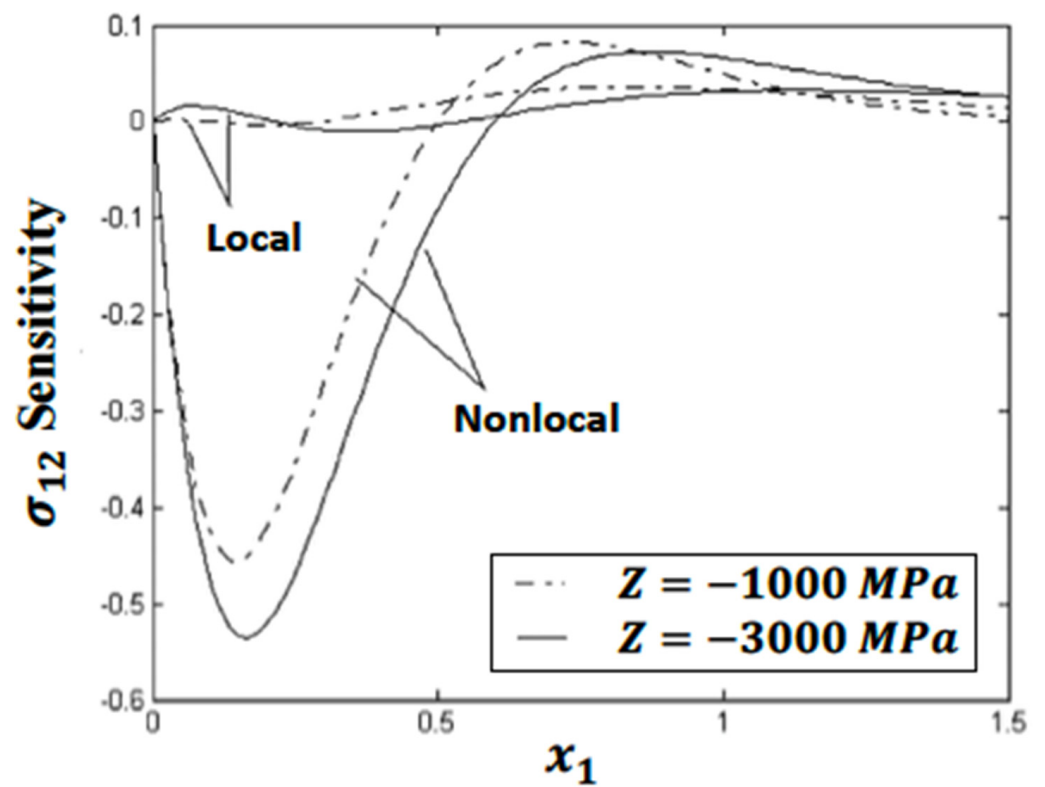

Figure 3. Variation in the thermal stress σ_{12} sensitivity along the x_1-axis for two different softening parameters of local and nonlocal theories.

Figure 4 depicts the behavior of the values of the stress σ_{22} sensitivity based on the softening parameters $Z = -1000$ MPa and $Z = -3000$ MPa for local and nonlocal theories, which are similar. The values of the stress σ_{22} sensitivity based on the softening parameter $Z = -1000$ MPa increase in the range $0 \leq x_1 \leq 1.5$. However, the values of the stress σ_{22} sensitivity based on the softening parameter $Z = -3000$ MPa increase in the range $0.15 \leq x_1 \leq 1.5$. The values of softening parameters $Z = -1000$ MPa and $Z = -3000$ MPa converge to zero with increasing distance x_1 at $x_1 \geq 1.5$.
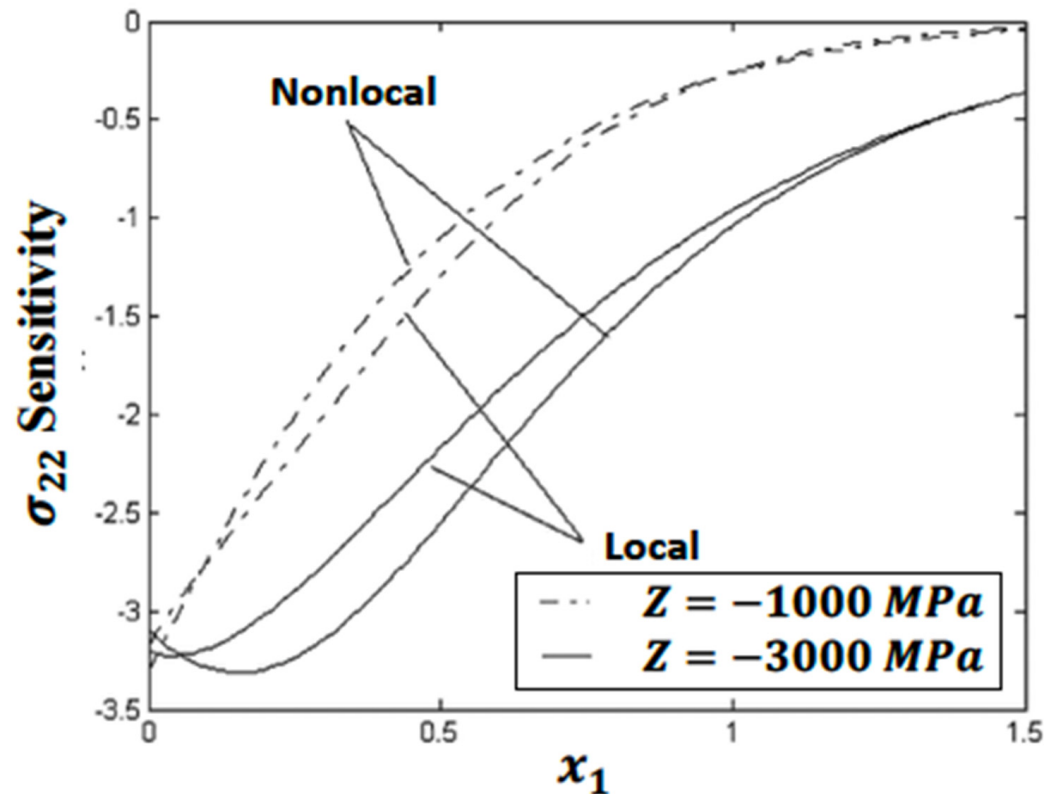

Figure 4. Variation in the thermal stress σ_{22} sensitivity along the x_1-axis for two different softening parameters of local and nonlocal theories.

There were no published results that supported the suggested technique's conclusions. Some of the literature can be considered as part of the planned investigation [42–46]. As a result, we examined a specific instance in our research and compared our BEM results to the finite difference method (FDM) and finite element method (FEM).

Figures 5–7 depict the distributions of the thermal stresses σ_{11}, σ_{12}, and σ_{22} overtime for the current BEM, finite difference method (FDM) of Ricci and Brünig [47], and the finite element method (FEM) of Su et al. [48]. These statistics demonstrate that the BEM is in excellent agreement with the SRBNS and FEM, proving the validity and accuracy of our suggested approach. The computing results for the considered problem were obtained using Matlab R2022a on a MacBook Pro with a 2.9 GHz Core i9 processor. The boundary element technique described in this paper applies to a wide variety of nonlocal thermo-elasto-plastic damage scenarios.
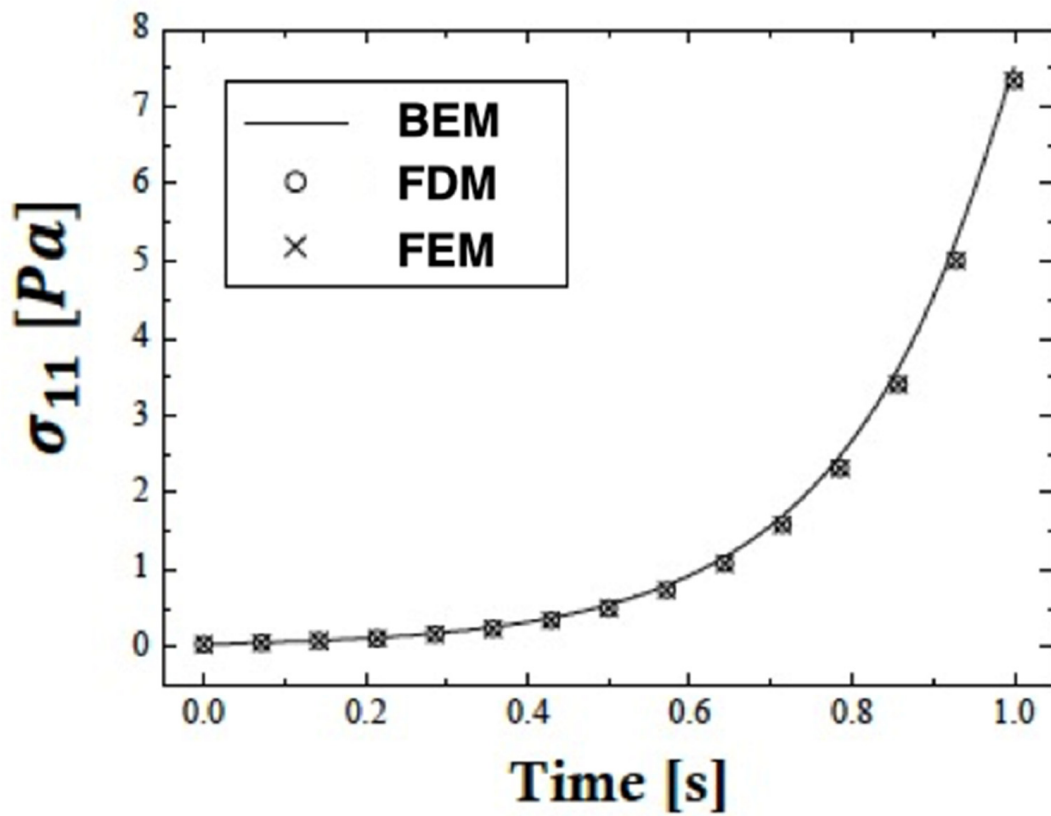
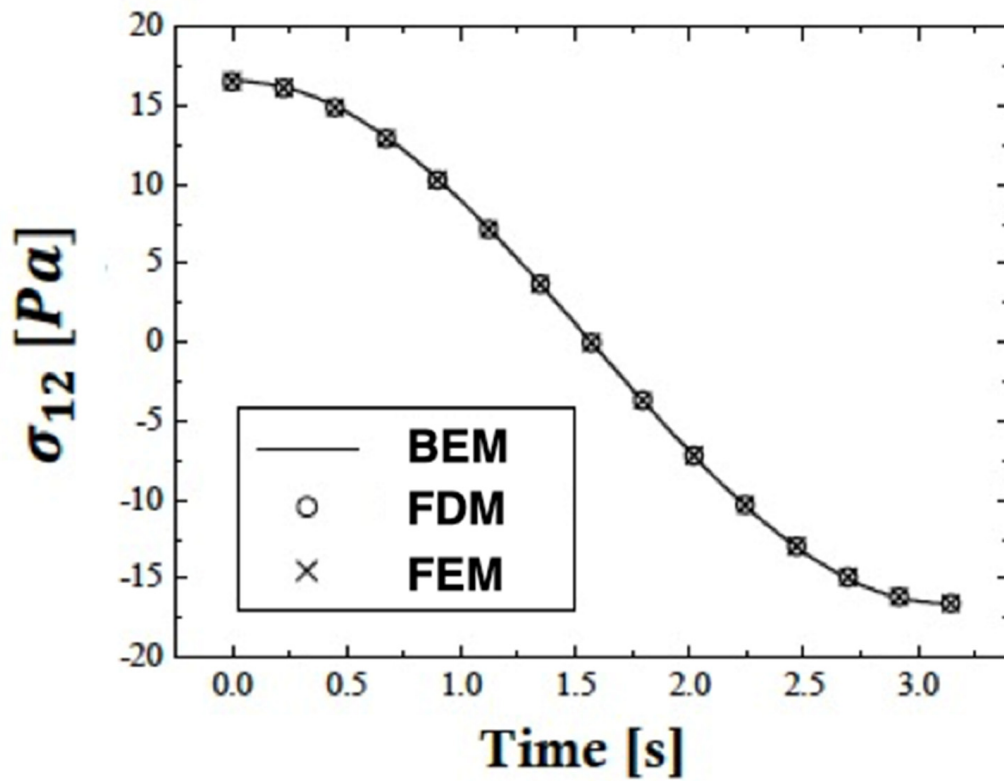**Figure 5.** Variation in the thermal stress σ_{11} with time for different methods.

Figure 6. Variation in the thermal stress σ_{12} with time for different methods.
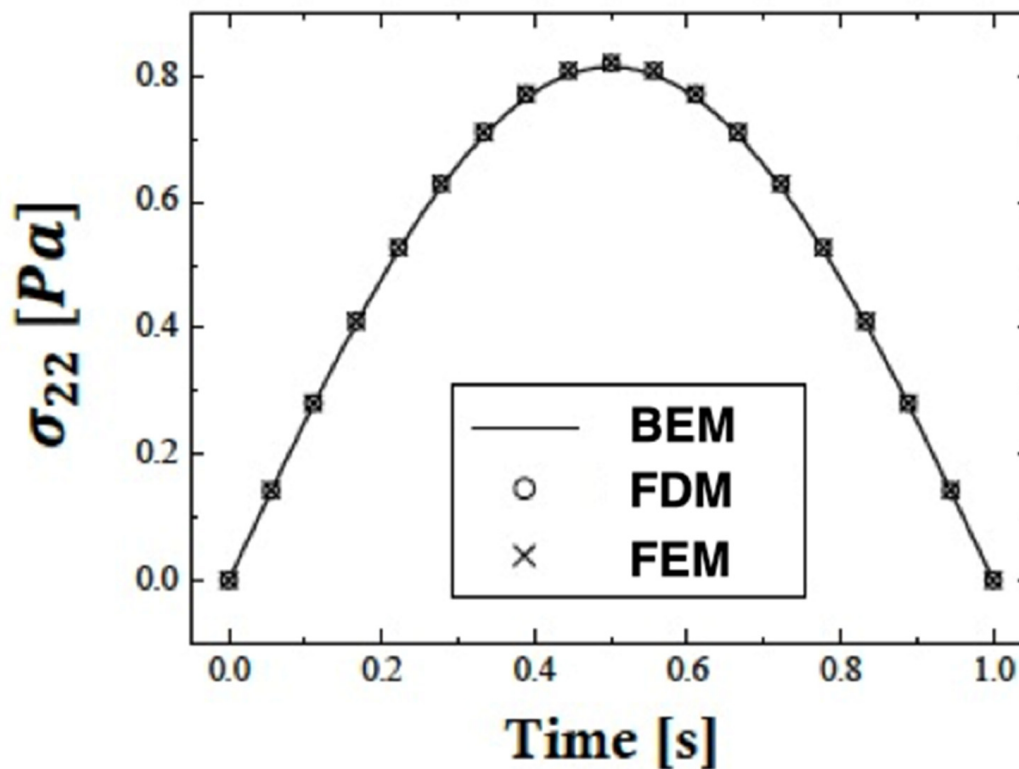
Figure 7. Variation in the thermal stress σ_{22} with time for different methods.

Table 2 compares the computer resources required to model the stress sensitivity of nonlocal thermo-elasto-plastic damage problems using BEM, FDM [47], and FEM [48]. This table demonstrates that the proposed BEM is more precise and efficient than both the FDM and the FEM.

Table 2. A comparison of the computer resources required to model stress sensitivity of nonlocal thermo-elasto-plastic damage problems.

	BEM	**FDM**	**FEM**
Number of nodes	50	50,000	45,000
Number of elements	25	15,000	13,000
CPU time [min.]	3	150	130
Memory [Mbyte]	1	130	110
Disc space [Mbyte]	0	190	170
Accuracy of results [%]	1.0	2.6	2.4

6. Conclusions

The numerical solution of the stress sensitivity in nonlocal thermo-elasto-plastic damage problems is presented using a new boundary element method (BEM) model. A boundary element model is used to represent the numerical solution to the heat conduction equation under non-local conditions. The non-local condition specifies the overall quantity of thermal energy contained in the substance under examination. The approach for solving the heat equation will disclose an unknown control function that governs the temperature in a specific section of the solid's boundary. The initial-stress BEM for structures with strain-softening damage is used in a boundary element program with iterations at each load increment to create a plasticity model with yield limit deterioration. To eliminate the challenges associated with the numerical calculation of singular integrals, the regularization technique is applicable to integral operators. A numerical scenario is used to validate the physical accuracy and efficiency of the proposed formulation.

Data Availability Statement: All data generated or analyzed during this study are included in this published article.

Conflicts of Interest: The authors declare no conflicts of interest.

Nomenclature

$\alpha(x, y)$	Nonlocal weight function	Ω	Domain
Γ	Boundary	$\psi(k)$	Work-hardening function
$\delta(s)$	Dirac delta function of argument s	CPV	Cauchy principal value
$\varepsilon(\tau)$	Total heat energy	c	Solid specific heat capacity
ε^P	Plastic strain intensity	c_{ijkl}	Tensor depending on the stress tensor
$\dot{\varepsilon}_{ij}^P$	Plastic strain rate	$dA(x, y)$	Area of an infinitesimal portion of Ω
$d\varepsilon_{ij}^P$	Plastic strain increment	$ds(x, y)$	Length of an infinitesimal part of Γ
θ	Temperature	E	Second kind elliptic integral
θ_0	Absolute zero temperature	$f\left(\sigma_{ij}\right)$	Effective stress σ_{e}
$\partial\theta/\partial n$	Outward normal derivative of θ on Γ	$\boldsymbol{I}$	Identity matrix
κ	Solid thermal conductivity	K	First kind elliptic integral
$\mu \text{ and } \lambda_{\mathrm{e}}$	Lamé elastic constants	k	hardening-softening parameter
$D\lambda$	Proportionality coefficient	l	Material characteristic length
$d\bar{\lambda}$	Spatial non-local average	$n_z^{(k)}$	z component unit vector normal to $\Gamma^{(k)}$
σ_{e}	Elastic stress intensity	$p(\tau)$	Control function
$\dot{\sigma}_{ij}$	Stress rate tensor	R	Solid Volume
$\dot{\sigma}_{ij}^P$	Plastic stress rate	(r, θ, z)	Cylindrical Coordinates
$\dot{\sigma}_{ij}^e$	Elastic stress rate	S	Solid Surface
$d\sigma_{ij}^e$	Elastic stress increment	s_{ij}	Deviator of stresses
$d\bar{\sigma}_{ij}^P$	Plastic stress increment	$\dot{t}_i$	Traction rate
$\tau(\eta)$	Unit vector tangent to boundary Γ at η	U_{ij}	Fundamental displacement
		$\dot{u}_i$	Displacement rate

References

1. Noye, B.J.; Dehghan, M.; VanderHoek, J. Explicit finite difference methods for two-dimensional diffusion with a non-local boundary condition. *Int. J. Eng. Sci.* **1994**, *32*, 1829–1834. [CrossRef]
2. Gumel, A.B.; Ang, W.T.; Twizell, E.H. Efficient parallel algorithm for the two-dimensional diffusion equation subject to specification of mass. *Int. J. Comput. Math.* **1997**, *64*, 153–163. [CrossRef]
3. Dehghan, M. Numerical solution of a parabolic equation subject to specification of energy. *Appl. Math. Comput.* **2004**, *149*, 31–45. [CrossRef]
4. Ang, W.T.; Ooi, E.H. A dual-reciprocity boundary element approach for solving axisymmetric heat equation subject to specification of energy. *Eng. Anal. Bound. Elem.* **2008**, *32*, 210–215. [CrossRef]
5. Bažant, Z.P. Instability, ductility and size effect in strain softening concrete. *J. Eng. Mech. Div. (ASCE)* **1976**, *12*, 331–344. [CrossRef]
6. Sandler, I.S. Strain-softening for static and dynamic problems. In *Proceedings of the Symposium on Constitutive Equations: Micro, Macro and Computational Aspects*; Willam, K.J., Ed.; ASME: New York, NY, USA, 1984; pp. 217–231.
7. Bažant, Z.P.; Lin, F.-B. Non-local yield degradation. *Int. J. Numer. Methods Eng.* **1988**, *26*, 1805–1823. [CrossRef]
8. Bažant, Z.P.; Belytschko, T.B.; Chang, T.P. Continuum theory for strain-softening. *J. Eng. Mech. Div. (ASCE)* **1984**, *110*, 1666–1692. [CrossRef]
9. Bažant, Z.P. Crack band model for fracture of geomaterials. In Proceedings of the 4th International Conference on Numerical Methods in Geomechanics, Edmonton, AB, Canada, 31 May–4 June 1982; Eisenstein, Z., Ed.; pp. 1137–1152.
10. Bažant, Z.P.; Ožbolt, J. Nonlocal microplane model for fracture, damage and size effect in structures. *J. Eng. Mech. (ASCE)* **1990**, *116*, 2485–2505. [CrossRef]
11. Bažant, Z.P.; Ožbolt, J. Compression failure of quasibrittle material; Nonlocal microplane model. *J. Eng. Mech. (ASCE)* **1992**, *118*, 540–556. [CrossRef]
12. Bažant, Z.P.; Cedolin, L. *Stability of Structures*; Oxford University Press: Oxford, UK, 1991.
13. Bažant, Z.P.; Planas, J. *Fracture and Size Effect in Concrete and Other Quasibrittle Materials*; CRC Press: Boca Raton, FL, USA, 1998.
14. Kröner, E. Elasticity theory of materials with long-range cohesive forces. *Int. J. Solids Struct.* **1967**, *4*, 731–742. [CrossRef]
15. Eringen, A.C.; Edelen, D.G.B. On nonlocal elasticity. *Int. J. Eng. Sci.* **1972**, *10*, 233–248. [CrossRef]

16. Bažant, Z.P.; Pijaudier-Cabot, G. Modeling of distributed damage by nonlocal continuum with local strain. In Proceedings of the 4th International Conference on Numerical Methods in Fracture Mechanics, San Antonio, TX, USA, 23–27 March 1987; pp. 411–432.

17. Pijaudier-Cabot, G.; Bažant, Z.P. Nonlocal damage theory. *J. Eng. Mech. (ASCE)* **1987**, *113*, 1512–1533. [CrossRef]

18. Jirásek, M. Nonlocal models for damage and fracture: Comparison of approaches. *Int. J. Solids Struct.* **1998**, *35*, 4133–4145. [CrossRef]

19. Bažant, Z.P.; Jirásek, M. Nonlocal integral formulations of plasticity and damage: Survey of progress. *J. Eng. Mech. (ASCE)* **2002**, *128*, 1119–1149. [CrossRef]

20. Swedlow, J.L.; Cruse, T.A. Formulation of boundary integral equations for three-dimensional flow. *Int. J. Solids Struct.* **1971**, *7*, 1673–1683. [CrossRef]

21. Ricardella, P.C. An Implementation of the Boundary Integral Technique for Planar Problems of Elasticity and Elasto-Plasticity. Ph.D. Thesis, Carnegie-Mellon University, Pittsburgh, RI, USA, 1973.

22. Chaudonneret, M. Boundary integral equation method for visco-plasticity analysis. *J. Mécanique Appliquée* **1977**, *1*, 113–131.

23. Kumar, V.; Mukherjee, S. A boundary integral equation formulation for time dependent inelastic deformation in metals. *Int. J. Mech. Sci.* **1975**, *19*, 713–724. [CrossRef]

24. Banerjee, P.K.; Cathie, D.N.; Davies, T.G. Two and three-dimensional problems of elastoplasticity. In *Developments in Boundary Element Methods*; Applied Science Publishers: London, UK, 1979; Volume 1, pp. 63–95.

25. Banerjee, P.K.; Cathie, D.N. Boundary element methods for axisymmetric plasticity. In *Innovative Numerical Methods for the Applied Engineering Science*; Shaw, R.P., Pilkey, W., Pilkey, B., Wilson, R., Lakis, A., Chaudouet, A., Marino, C., Eds.; University of Virginia Press: Charlottesville, VA, USA, 1980.

26. Telles, J.C.F.; Brebbia, C.A. Boundary elements in plasticity. *Appl. Math. Model.* **1981**, *5*, 275–281. [CrossRef]

27. Henry, D.P.; Banerjee, P.K. A new BEM formulation for two and three-dimensional elastoplasticity using particular integrals. *Int. J. Numer. Methods Eng.* **1988**, *26*, 2079–2096. [CrossRef]

28. Leitao, V.; Alabadi, M.H.; Rooke, D.P. The dual boundary element formulation for elastoplastic fracture mechanics. *Int. J. Numer. Methods Eng.* **1995**, *38*, 315–333. [CrossRef]

29. Herding, U.; Kuhn, G. A field boundary element formulation for damage mechanics. *Eng. Anal. Bound. Elem.* **1996**, *18*, 137–147. [CrossRef]

30. Balaš, J.; Sládek, J.; Sládek, V. *Stress Analysis by Boundary Element Methods*; Elsevier: Amsterdam, The Netherlands, 1989.

31. Brebbia, C.A.; Telles, J.C.F.; Wrobel, L.C. *Boundary Element Techniques, Theory and Applications in Engineering*; Springer: Berlin/Heidelberg, Germany, 1984.

32. Abramowitz, M.; Stegun, I. *Handbook of Mathematical Functions*; Dover: New York, NY, USA, 1970.

33. París, F.; Cañas, J. *Boundary Element Method: Fundamentals and Applications*; Oxford University Press: Oxford, UK, 1997.

34. Wang, K.; Mattheij, R.M.M.; ter Morsche, H.G. Alternative DRM formulations. *Eng. Anal. Bound. Elem.* **2003**, *27*, 175–181. [CrossRef]

35. Sládek, J.; Sládek, V.; Bažant, Z.P. Non-local boundary integral formulation for softening damage. *Int. J. Numer. Methods Eng.* **2003**, *57*, 103–116. [CrossRef]

36. Sládek, V.; Sládek, J. Non-singular boundary integral representation of stresses. *Int. J. Numer. Methods Eng.* **1992**, *33*, 1481–1499. [CrossRef]

37. Sládek, V.; Sládek, J. Displacement gradients in BEM formulation for small strain plasticity. *Eng. Anal. Bound. Elem.* **1999**, *23*, 471–477. [CrossRef]

38. Tanaka, M.; Sládek, V.; Sládek, J. Regularization techniques applied to boundary element methods. *Appl. Mech. Rev. (ASME)* **1994**, *47*, 457–499. [CrossRef]

39. Xu, Z.; Alonso, J.J.; Darve, E. A numerically stable communication avoiding S-step GMRES algorithm. *arXiv* **2023**, arXiv:2303.08953. [CrossRef]

40. Shao, X.H.; Kang, C.B. Modified DTS iteration methods for spatial fractional diffusion equations. *Mathematics* **2023**, *11*, 931. [CrossRef]

41. She, Z.H.; Qiu, L.M.; Qu, W. An unconditionally convergent RSCSCS iteration method for Riesz space fractional diffusion equations with variable coefficients. *Math. Comput. Simul.* **2023**, *203*, 633–646. [CrossRef]

42. Fahmy, M.A. Shape design sensitivity and optimization for two-temperature generalized magneto-thermoelastic problems using time-domain DRBEM. *J. Therm. Stress.* **2018**, *41*, 119–138. [CrossRef]

43. Fahmy, M.A. Shape design sensitivity and optimization of anisotropic functionally graded smart structures using bicubic B-splines DRBEM. *Eng. Anal. Bound. Elem.* **2018**, *87*, 27–35. [CrossRef]

44. Fahmy, M.A.; Alsulami, M.O. Boundary Element and Sensitivity Analysis of Anisotropic Thermoelastic Metal and Alloy Discs with Holes. *Materials* **2022**, *15*, 1828. [CrossRef] [PubMed]

45. Fahmy, M.A. Three-Dimensional Boundary Element Strategy for Stress Sensitivity of Fractional-Order Thermo-Elastoplastic Ultrasonic Wave Propagation Problems of Anisotropic Fiber-Reinforced Polymer Composite Material. *Polymers* **2022**, *14*, 2883. [CrossRef] [PubMed]

46. Fahmy, M.A.; Alsulami, M.O.; Abouelregal, A.E. Sensitivity analysis and design optimization of 3T rotating thermoelastic structures using IGBEM. *AIMS Math.* **2022**, *7*, 19902–19921. [CrossRef]

47. Ricci, S.; Brünig, M. Numerical Analysis of Nonlocal Anisotropic Continuum Damage. *Int. J. Damage Mech.* **2007**, *16*, 283–299. [CrossRef]
48. Su, C.; Lu, D.; Zhou, X.; Wang, G.; Zhuang, X.; Du, X. An implicit stress update algorithm for the plastic nonlocal damage model of concrete. *Comput. Methods Appl. Mech. Eng.* **2023**, *414*, 116189. [CrossRef]